A NUSTAR OBSERVATION OF THE GAMMA-RAY EMITTING MILLISECOND PULSAR PSR J1723–2837

A. K. H. KONG[1,2], C. Y. HUI[3], J. TAKATA[4], K. L. LI[5], P. H. T. TAM[6]

[1] Institute of Astronomy and Department of Physics, National Tsing Hua University, Hsinchu 30013, Taiwan; akong@phys.nthu.edu.tw
[2] Astrophysics, Department of Physics, University of Oxford, Keble Road, Oxford OX1 3RH, UK
[3] Department of Astronomy and Space Science, Chungnam National University, Daejeon, Republic of Korea; cyhui@cnu.ac.kr
[4] Institute of Particle Physics and Astronomy, Huazhong University of Science and Technology, China
[5] Department of Physics and Astronomy, Michigan State University, East Lansing, MI 48824, USA and
[6] Institute of Astronomy and Space Science, Sun Yat-Sen University, Guangzhou 510275, China
Accepted for publication in ApJ

ABSTRACT

We report on the first *NuSTAR* observation of the gamma-ray emitting millisecond pulsar binary PSR J1723–2837. X-ray radiation up to 79 keV is clearly detected and the simultaneous *NuSTAR* and *Swift* spectrum is well described by an absorbed power-law with a photon index of ~ 1.3. We also find X-ray modulations in the 3–10 keV, 10–20 keV, 20–79 keV, and 3–79 keV bands at the 14.8-hr binary orbital period. All these are entirely consistent with previous X-ray observations below 10 keV. This new hard X-ray observation of PSR J1723–2837 provides strong evidence that the X-rays are from the intrabinary shock via an interaction between the pulsar wind and the outflow from the companion star. We discuss how the *NuSTAR* observation constrains the physical parameters of the intrabinary shock model.

Keywords: binaries: close—pulsars: individual (PSR J1723–2837)—X-rays: binaries

1. INTRODUCTION

Thanks to the combined effort of continuous $\gamma-$ray all-sky observation and radio pulsation searches, the population of millisecond pulsars (MSPs) are expanded significantly in the recent years (see the review by Hui 2014). Among these newly discovered MSPs, one interesting new class which is usually referred as "redbacks" has emerged. They are characterized by their non-degenerate companions with the mass ranges from $\sim 0.2 M_\odot$ to $\sim 0.7 M_\odot$ and with the orbital period $P_b \lesssim 20$ hrs (see Roberts 2013 for a review).

The first discovered redback MSP PSR J1023+0038 has provided us with the long-sought evidence of a compact binary transiting from an accretion-powered state to a rotation-powered state (Archibald et al. 2009). Theoretical models (Shvartsman 1970; Burderi et al. 2001) have also suggested that these systems can swing between the rotation-powered and accretion-power states according to the mass transfer rate. Such behavior has also been firstly seen in PSR J1023+0038 with the disappearance of radio pulsations (Stappers et al. 2013; Patruno et al. 2014), a newly formed accretion disk (Halpern et al. 2013) and the dramatic increase of UV, X-ray and $\gamma-$ray emission (Li et al. 2014).

In this investigation, we focus on another redback MSP PSR J1723–2837. Its spin period and spin-down rate are $P \sim 1.86$ ms and $\dot{P} \sim 7.5 \times 10^{-21}$ s s^{-1} respectively (Crawford et al. 2013). This implies a spin-down power of $\dot{E} \sim 4.6 \times 10^{34}$ erg s^{-1}. Its distance inferred from the dispersion measure is $d \sim 750$ pc, which makes it the closest redback that has been found in the Galactic field so far [1].

PSR J1723–2837 is in a binary orbit with a period of $P_b \sim 14.8$ hr. Its companion is a G-type star companion with the mass in a range of $0.4 - 0.7$ $M_\odot$ (Crawford et al. 2013). The orbit is almost circular with the projected semi-major axis of $a \sim 1.23$ lt-s. The interval of radio eclipse has covered $\sim 15\%$ of the orbit (Crawford et al. 2013). Through a long-term optical photometry of PSR J1723–2837, van Staden & Antoniadis (2017) have found that the companion and the pulsar are not tidally locked.

No $\gamma-$ray counterpart of PSR J1723–2837 was found in the second *Fermi* point source catalog (2FGL; Nolan et al. 2012). Hui et al. (2014) have searched for the $\gamma-$ray emission from PSR J1723–2837 with ~ 3 years of *Fermi* data and found a possible counterpart of $\sim 6\sigma$ at the pulsar position. While this source is not in the 2FGL catalog, an unidentified source 1FGL J1725.5–2832 in the first *Fermi* catalog (Abdo et al. 2010) is found in the proximity of the pulsar (see Fig. 3 in Hui et al. 2014). Since it is $\lesssim 1°$ away from the pulsar and its $\gamma-$ray properties are consistent with those found by Hui et al. (2014), the authors suggest 1FGL J1725.5–2832 is the same $\gamma-$ray source associated with PSR J1723–2837. In the latest third *Fermi* catalog (Acero et al. 2015), a source, 3FGL J1725.1-2832, is also found to be associated with 1FGL J1725.5–2832 and its flux and spectrum is fully consistent with the possible gamma-ray counterpart of PSR J1723–2837.

Hui et al. (2014) have also examined the X-ray properties of PSR J1723–2837 with *XMM-Newton* and *Chandra*. They have discovered the orbital modulation in $0.3 - 10$ keV with the minimum coincides with the phase interval of radio eclipses. Its phase-averaged X-ray spectrum is purely non-thermal and can be modeled by a simple power-law with $\Gamma \sim 1.2$. No significant spectral variation across the orbit is found in this investigation. The authors have discussed the X-ray properties in the contest of an intrabinary shock model. Assuming a synchrotron origin of the X-rays, Hui et al. (2014) speculated if typical synchrotron energy is larger than

---

[1] For updated information, please refer to https://apatruno.wordpress.com/about/millisecond-pulsar-catalogue/

~ 10 keV. However, this scenario could not be examined in their work because both *XMM-Newton* and *Chandra* cannot provide spectral imaging data in the hard X-ray band.

In this paper, we report a broadband X-ray analysis of PSR J1723–2837 with photon energies up to ~ 79 keV by using the data obtained from *NuSTAR*. This is also the second redback MSP observed with *NuSTAR* after PSR J1023+0038 (Tendulkar et al. 2014; Li et al. 2014).

2. OBSERVATIONS AND DATA REDUCTION

2.1. *NuSTAR*

PSR J1723–2837 was observed with *NuSTAR* (Harrison et al. 2013) between 2015 October 15 and 17 with an effective exposure time of ~ 81 ks (ObsID 30101043002). We reprocessed the raw data with the *NuSTAR* Data Analysis Software (NuSTARDAS) v1.7.0 under HEAsoft version 6.20 and an updated NuSTAR calibration data (CALDB version 20170120). The calibrated and and cleaned event files were produced with `nupipeline`. All the data products including images, light curves, X-ray spectra and the corresponding response matrices were generated by the tool `nuproducts`.

We cleaned and filtered the events with standard parameters suggested in the *NuSTAR* Data Analysis Software Guide[2]. Both focal plane modules, FPMA and FPMB, were processed separately to extract the data products. In addition to standard processing, we also performed barycentric correction with the tool `barycorr` to the arrival times of all events based on the pulsar timing position at R.A. (J2000) = 17:23:23.1856, Decl. = -28:37:57.17 (Crawford et al. 2013).

The X-ray counterpart of PSR J1723–2837 is clearly detected in both modules. Apart from PSR J1723–2837, a faint known X-ray source, 3XMM J172325.7–283631 (in 3XMM-DR6 catalog), is also detected at ~ 1.5 arcmin northeast to PSR J1723–2837. This faint source is nearly a factor of 10 fainter than PSR J1723–2837.

To extract events for spectral and temporal analysis, we used data only in the range of 3–79 keV. We employed a circular region with a radius of 50 arcsec centered at the position of PSR J1723–2837. A circular source-free region on the same detector chip was used for background subtraction. The X-ray spectra of the source extracted from FPMA and FPMB were rebinned to have at least 30 counts per bin.

2.2. *Swift*

Three *Swift* snapshot observations with a total exposure time of about 5.3 ks were taken simultaneously with the *NuSTAR* observation. In this study, we use the imaging data taken with the X-ray Telescope (XRT) onboard *Swift* to constrain the soft (< 3 keV) X-ray emission. We extracted the co-added X-ray spectrum (to improve the signal-to-noise ratio) and the corresponding response files by using the XRT products generator [3] (Evans et al. 2007,2009).

## 3. DATA ANALYSIS

3.1. *Timing Analysis*
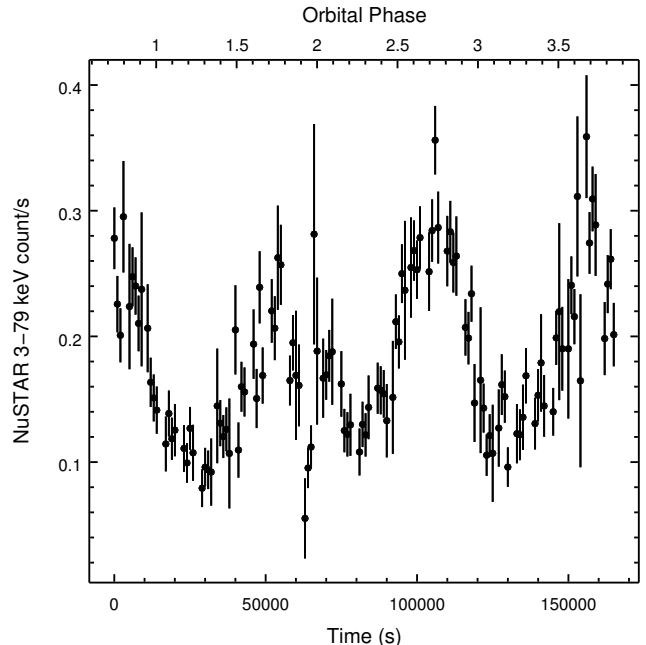
Figure 1. Background subtracted *NuSTAR* 3–79 keV light curve of PSR J1723–2837. Each bin corresponds to 1000 s of exposure time.

PSR J1723–2837 is known to have a 14.8-hr X-ray orbital period using *Chandra* and *XMM-Newton* observations (Hui et al. 2014). To search for the hard X-ray orbital modulation with *NuSTAR*, we combined the background subtracted light curves from FPMA and FPMB (Figure 1). In addition to the 3–79 keV light curve, we also extracted light curves from 3–10 keV, 10–20 keV, and 20–79 keV. Using the radio timing ephemeris (Crawford et al. 2013), we folded the barycentered events at the orbital period (Figure 2). The phase zero is defined as the time of the ascending node (MJD 55425.320466), meaning that the inferior conjunction (when the companion star is between the pulsar and observer) is at phase 0.25. The orbital period is clearly shown in all energy ranges concerned. The profiles of the light curves are similar to that of *Chandra* and *XMM-Newton* (Hui et al. 2014), and the minimum of the X-ray light curves (at phase ~ 0.25) corresponds to the radio eclipse (Crawford et al. 2013). We also computed the ratios between different energy bands and there is no evidence of color variation throughout the orbital period (see Figure 2 for the flux ratio between 20–79 keV and 3–10 keV) and we will show in section 3.2 that the phase-resolved spectral fits of the minimum and maximum are statistically the same.

Furthermore, the X-ray light curves show a dipping feature on a timescale of about 3 hours in one occasion (see Figure 1). This feature happened in between the maximum and minimum of the light curve at the orbital phase of ~ 0.9. To test the significance, we fit the light curve with a 14.8-hr sinusoidal plus a Gaussian centered at the dip. The addition of the Gaussian is significant at $> 99.9\%$ level by using an F-test. We also checked the light curves in different energy bands and this feature may be seen in all bands, but it is statistically significant ($> 99.9\%$) only in the 3–10 keV band. For the other bands, the small numbers of photons do not allow us to
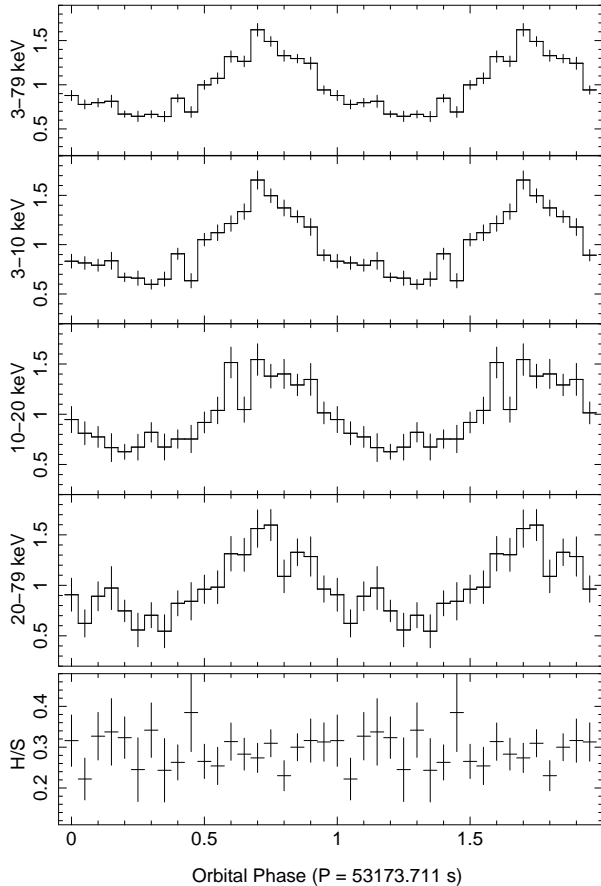
Figure 2. Folded light curves at different energy bands of PSR J1723–2837 with an orbital period of 53173.711 s. From top to bottom: 3–79 keV, 3–10 keV, 10–20 keV, 20–79 keV, and hardness ratio (20-79 keV / 3–10 keV). It is clear that all light curves show the 14.8-hr orbital period. The hardness ratio remains steady throughout the orbital period, indicating that there is no color variation.

claim a detection. The hardness ratio did not reveal any variability.

3.2. *Spectral Analysis*

We performed spectral analysis using XSPEC version 12.9.1. We first fit the phase-averaged spectrum with a simple absorbed power-law model. This is based on the fact that there is no indication of any thermal emission from the 0.3–10 keV spectra (Hui et al. 2014). To constrain the soft X-rays below 3 keV (where *NuSTAR* is not sensitive), we performed a joint fit together with the simultaneous *Swift*/XRT data. We also included constants to take cross-calibration between *NuSTAR* FPMA and FPMB and *Swift*/XRT into account. Figure 3 shows the broadband energy spectrum of PSR J1723–2837. The spectrum clearly extends up to about 70 keV with no significant emission and absorption features and can be well described by an absorbed power-law model ($\chi_\nu^2 = 0.87$ for 289 degrees of freedom (dof)). The best-fit model parameters are $N_H = (3.9^{+2.7}_{-2.0}) \times 10^{21}$ cm^{-2} and $\Gamma = 1.28 \pm 0.04$. All quoted uncertainties in this paper are 90% confidence level. The best-fit N_H is entirely consistent with the Galactic value ($\sim 4 \times 10^{21}$ cm^{-2}; Kalberla et al. 2005). The unabsorbed 3–79 keV flux is
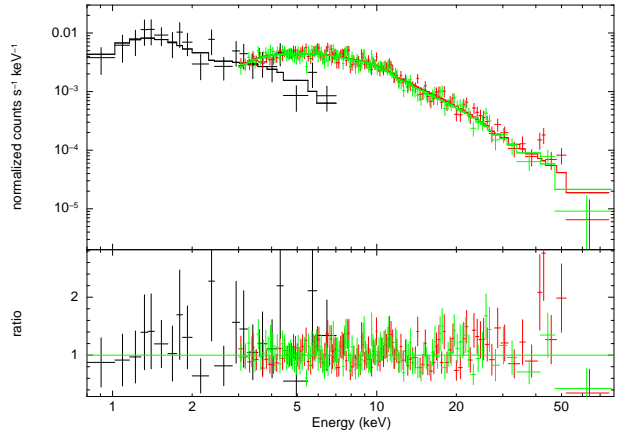
Figure 3. Broadband phase-averaged spectrum of PSR J1723–2837 taken with *Swift*/XRT (black data points and line) and *NuSTAR* (red and green data points and lines). The best-fit spectrum is an absorbed power-law with $N_H = 3.9 \times 10^{21}$ cm^{-2} and $\Gamma = 1.28$.

$(9.6 \pm 0.5) \times 10^{-12}$ ergs cm^{-2} s^{-1}, corresponding to an X-ray luminosity of $(6.5 \pm 0.3) \times 10^{32}$ ergs s^{-1} ($d = 0.75$ kpc).

We also fit the spectrum with a power-law model with a high-energy exponential cutoff. However, the fit was not improved significantly and the cutoff energy is unreasonably large (> 300 keV). We therefore conclude that a simple power-law model is sufficient to describe the spectrum.

We next investigated two phase-resolved spectra covering the orbital phase of 0.2–0.4 and 0.7–0.9. These two phase ranges roughly corresponds to the X-ray minimum (inferior conjunction) and maximum (superior conjunction), respectively. For the phase-resolved spectroscopy, we used the *NuSTAR* data only since the *Swift* observations do not have sufficient photons. We fixed the N_H at the best-fit value determined from the phase-averaged spectrum. The best-fit Γ is 1.32 ± 0.12 and 1.25 ± 0.06 for inferior and superior conjunction, respectively. Varying the N_H within the 90% uncertainty gives consistent results. This shows that both spectra are statistically the same and are consistent with the phase-averaged spectrum. We conclude that there is no significant X-ray spectral variability throughout the binary orbit of PSR J1723–2837. The *NuSTAR* results are in general consistent with *Chandra* and *XMM-Newton* observations but for the superior conjunction, the spectrum of *NuSTAR* is steeper than that of *Chandra*/*XMM-Newton*.

4. DISCUSSION

We have investigated hard X-ray (3–79 keV) properties of the MSP binary PSR J1723–2837 with *NuSTAR*. The 14.8-hr binary orbital period of the system is clearly shown in hard X-ray (Figure 1 and 2) and the profile is similar to that seen in *Chandra* and *XMM-Newton* (Hui et al. 2014). The broadband (0.3–79 keV) energy spectrum from the joint *Swift* and *NuSTAR* data shows an absorbed power-law with $\Gamma = 1.28$ and an X-ray (3–79 keV) luminosity of 6.5×10^{32} ergs s^{-1}. The *NuSTAR* results strongly support the non-thermal nature of the X-ray emission as already indicated in previous studies with *Chandra* and *XMM-Newton* (Hui et al. 2014). To produce such a hard X-ray spectrum, it is suggested that the X-rays are from an intrabinary shock due to interac-

tion between pulsar wind and outflow from the companion star (Takata et al. 2014; Li et al. 2014). This model also explains the X-ray orbital modulation naturally.

The *NuSTAR* result is not only consistent with previous results based on soft ($<$ 10 keV) X-ray data, but also similar to the transitional redback MSPs PSR J1023+0038. PSR J1023+0038 is the first redback MSP observed with *NuSTAR* (Tendulkar et al. 2014; Li et al. 2014). During its rotation-powered state, PSR J1023+0038 shows a hard spectrum ($\Gamma = 1.2$) comparing to a relatively soft ($\Gamma = 1.7$) spectrum seen in a low-mass X-ray binary state. The hard X-ray luminosity of the two objects during their rotation-powered state is also the same. Interestingly enough, the GeV spectra of the two sources taken with *Fermi* are also very similar with a power-law photon index of $\sim$ 2.5 (Hui et al. 2014; Takata et al. 2014; Patruno et al. 2014). With the new information provided by *NuSTAR*, we here explain the X-ray emission of PSR J1723–2837 with a revised intrabinary shock model.

The orbit modulating X-rays of PSR J1723–2837 are likely produced by the intrabinary shock like other redback MSP binary such as PSR J1023+0038 (Takata et al. 2014; Li et al. 2014) and PSR J2339–0533 (Kong et al. 2012). The observed radio eclipse at several GHz lasts only 15% of its binary orbit, suggesting the shock wraps the companion star and its distance from the pulsar is of order of the orbit separation, which is of order of $a \sim 5 \times 10^{10}$cm (Crawford et al. 2013). The magnetic fields at the shock may be estimated as $B_s \sim (L_{sd}\sigma/a^2c)^{1/2} \sim 7.8$G, where we used $L_{sd} = 4.6 \times 10^{34}$erg s^{-1}, $a = 5 \times 10^{10}$cm and $\sigma = 0.1$ as the the ratio of the magnetic energy to the kinetic energy of the relativistic pulsar wind (Takata et al. 2017). At the shock, the kinetic energy of the pulsar wind is converted into the internal energy, and the pulsar wind particles are accelerated beyond the Lorentz factor of the cold relativistic pulsar wind in the upstream region. We may estimate the maximum Lorentz factor of the accelerated particle by balancing the accelerating time scale, $\tau_{acc} \sim \Gamma_{max}m_ec/(\zeta eB_s)$, where $\zeta < 1$ is the efficiency of shock acceleration, and synchrotron cooling time scale, $\tau_s \sim 9m_ec^3c^5/(4e^4B_s^2\Gamma_{max})$, which yields $\Gamma_{max} \sim 4 \times 10^7\zeta^{1/2}(B_s/10\text{G})^{-1/2}$. These TeV electrons accelerated at the shock will produce the very high-energy photons by scattering off the soft photons from the companion star ($T_{eff} \sim 4800 - 6000$K), which could possibly be measured by the Cherenkov Telescope Array (CTA) in the future.

For the synchrotron radiation, the process is oc-

curred in the fast-cooling regime for the shocked particles with a Lorentz factor above $\Gamma_c \sim 1.5 \times 10^6(a/5 \cdot 10^{10}\text{cm})^{-1}(B_s/10\text{G})^{-2}$, corresponding to the typical synchrotron photon energy of $E_{s,c} \sim 400$keV$(\Gamma_c/1.5 \cdot 10^6)^2(B_s/10\text{G})$. The photon index changes from $\alpha = (p+2)/2$ above $E_{s,c}$ to $\alpha = (p+1)/2$ below $E_{s,c}$. At the typical synchrotron energy (E_1) of the minimum Lorentz factor (Γ_1) of the shocked particles, the photon index changes from $\alpha = (p+1)/2$ above E_1 to $\alpha = 2/3$ below E_1. *Chandra*, *XMM-Newton*, and *NuSTAR* observations revealed that the X-ray emissions in 0.3–79 keV energy range is well described by a simple power-law with a photon index of $\sim$ 1.2 − 1.3, which is similar to the transitional MSP PSR J1023+0038. This simple power law spectrum may indicate that the typical synchrotron energy (E_1) of the minimum Lorentz factor Γ_1 is smaller than 0.1 keV, and the power law index of the particle distribution at the shock is $p \sim 1.4 - 1.6$. In such a case, the minimum Lorentz factor is constrained as $\Gamma_1 \leq 2.4 \times 10^4(B_s/10\text{G})^{-1/2}$.

Apart from the X-ray orbital modulation, the X-ray light curve also shows a short-term dipping feature on a timescale of about 3 hours in between the inferior and superior conjunctions. Given the orbital phase (~ 0.9) of the dip, it is unlikely due to an eclipse. The lack of a hardness change during the dip indicates that it may be intrinsic to the X-ray radiation (i.e., intrabinary shocked X-rays) caused by perturbation of shock front via clumpy pulsar wind or outflow variation from the companion. For instance, if the outflow velocity from the companion has a sudden drop, the momentum ratio of the stellar wind and the pulsar wind will drop accordingly, resulting a smaller fraction of the pulsar wind stopped by the outflow.

In summary, we found modulating X-ray radiation at the 14.8-hr binary orbit of PSR J1723–2837 up to 79 keV with *NuSTAR*. The energy spectrum is a simple power-law with a photon index of $\sim$ 1.3 and shows no evidence of spectral variability throughout the orbital cycle. Such radiation can be explained with an intrabinary shock model.

Facilities: NuSTAR, Swift

REFERENCES

Abdo, A.A. et al. 2010, ApJS, 188, 405
Acero, F. et al. 2015, ApJS, 218, 23
Archibald, A. M. et al. 2009, Science, 324, 1411
Burderi, L. et al. 2001, ApJ, 560, L71
Crawford, F. et al. 2013, ApJ, 776, 20
Evans, P. A. et al. 2007, A&A, 469, 379
Evans, P. A. et al. 2009, MNRAS, 397, 1177
Halpern, J. P., Gaidos, E., Sheffield, A., Price-Whelan, A. M., Bogdanov, S. 2013, ATel, 5514
Harrison, F. A. et al. 2013, ApJ, 770, 103
Hui, C. Y. 2014, Journal of Astronomy and Space Science, 31, 101
Hui, C. Y., Tam, P. H. T., Takata, J., Kong, A. K. H., Cheng, K. S., Wu, J. H. K., Lin, L. C. C., Wu, E. M. H. 2014, ApJ, 781, L21

Kalberla et al. 2005, Astronomy & Astrophysics, 440, 775
Kong, A. K. H., Huang, R. H. H., Cheng, K. S., Takata, J., Yatsu, Y., Cheung, C. C., Donato, D., Lin, L. C. C., Kataoka, J., Takahashi, Y., Maeda, K., Hui, C. Y., Tam, P. H. T. 2012, ApJ, 747, L3
Li, K.L., Kong, A.K.H., Takata, J., Cheng, K.S., Tam, P.H.T., Hui, C.Y., Jin, R. 2014, ApJ, 797, 111
Nolan, P.L., et al. 2012, ApJS, 199, 31
Patruno, A., Archibald, A. M., Hessels, J. W. T. et al. 2014, ApJ, 781, L3
Roberts, M. S. E. 2013, Proceedings of IAUS 291 "Neutron Stars and Pulsars: Challenges and Opportunities after 80 years", J. van Leeuwen (ed.), p.127

Stappers, B. W., Archibald, A. M., Hessels, J. W. T. et al. 2014, ApJ, 790, 39

Shvartsman, V. F. 1970, Radiophysics and Quantum Electronics, 13, 1428

Takata, J., Li, K. L., Leung, G. C. K., Kong, A. K. H., Tam, P. H. T., Hui, C. Y., Wu, E. M. H., Xing, Y., Cao, Y., Tang, S., Wang, Z., Cheng, K. S. 2014, ApJ, 785, 131

Takata, J., Tam, P. H. T., Ng, C. W., Li, K. L., Kong, A. K. H., Hui, C. Y., Cheng, K. S. 2017, ApJ, 836, 241

Tendulkar, S.P. et al. 2014, ApJ, 791, 77

van Staden, A.D., Antoniadis, J. 2017, ApJ, 833, L12